FAILURE ANALYSIS OF UNDERGROUND RC FRAME SUBJECTED TO SEISMIC ACTION

(Translation from Proceedings of JSCE, No.571/V-36, August 1997)

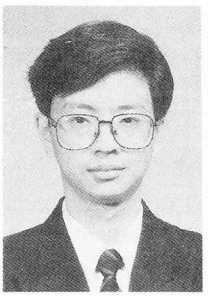

Xuehui AN

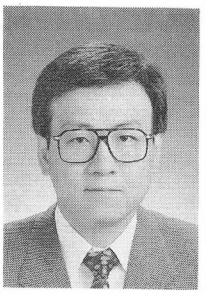

Koichi MAEKAWA

This paper describes failure analysis carried out on an underground RC frame. The Great Hanshin Earthquake in 1995 caused serious damage to RC subway station frames. To study the collapse mechanism, the seismic response of a subway station is simulated using the 2-D FEM program WCOMD-SJ, based on the path-dependent RC smeared crack model and models of the soil foundation and the interface. Shear failure of middle vertical columns is found to be the major cause of the structural collapse. Further, a parametric study of reinforcement ratio and foundation properties is implemented to investigate the seismic performance of underground RC culverts.

Key Words: *FEM, dynamic analysis, underground structure, RC, soil-structure interaction*

Xuehui AN is an engineer at Tokyo Electric Power Services Co., Ltd.. He obtained his D. Eng. from the University of Tokyo in 1996. He is a member of the JSCE.

Koichi MAEKAWA is a professor in the Dept. of Civil Engineering at the University of Tokyo. He obtained his D. Eng. from the University of Tokyo in 1985. He is a member of the JSCE.

---

1. INTRODUCTION

The Great Hanshin Earthquake on January 17, 1995 caused the disastrous collapse of many reinforced concrete structures, including some underground subway stations in Kobe city. As this was the first time catastrophic failure of underground structures was experienced, there is a great need to clarify the collapse mechanism of these underground frames and to update the seismic design standards if necessary.

In this study, a double-deck underground RC frame for a subway station is investigated to determine its failure mode and failure mechanism, and to examine computational tool for the further study of earthquake resistant design. The observed damage as reported in the literature[1,2] is compared with analytical results of verification method on which enhanced seismic resistant design will be based in future.

2. COMPUTATION TOOL

In this paper, the two dimensional FEM program WCOMD-SJ is used to analyze coupled reinforced concrete and soil structures under seismic excitation. The constitutive models for reinforced concrete, soil and the interface between soil, and RC are installed in the software.

In the model for reinforced concrete, the multi-directional smeared crack model of concrete is employed, and the constitutive law of reinforcing bar is composed. The concrete model consists of tension stiffening, compression, and shear transfer models. These models are given as the relationship between average stress and average strain in the reinforced concrete. The crack spacing, or density, and reinforcing bar diameter have a negligible effect on the spatially average stress-strain relation defined on a RC control volume, as shown in **Fig.1a**[3,4]. The continuum damage model of concrete encompasses the reduced compressive capacity of cracked concrete in relation to the strain normal to the crack[5].

A path-dependent constitutive model for soil is essential in dealing with the kinematic interactions of the entire RC-soil system under strong seismic loading, as shown in **Fig.1b**[6]. Here, Ohsaki's model[7] defines the formula for the envelope expressing the nonlinear shear stress-strain relation for soil. The internal loops represent Masing's rule. In addition, separation and sliding between soil and the structure are taken into account along the interfacial zone as shown in **Fig.1c**.

The full path-dependent constitutive models were integrated in the scheme of Newmark step-by-step direct integration scheme for both time and strain histories. In this way, the dynamic nonlinear response of the RC-soil structure can be computed within a versatile computational scheme.

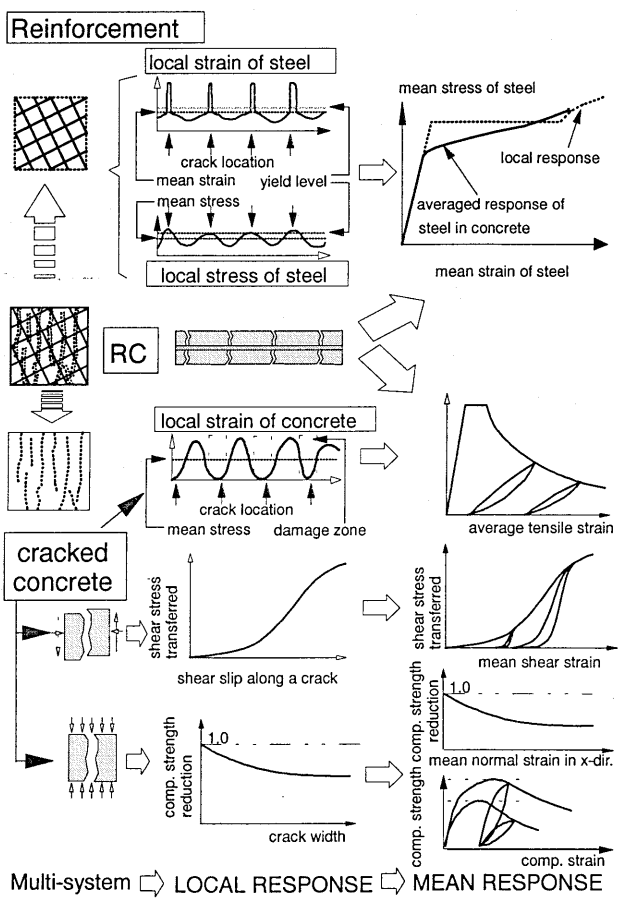

Fig.1a Constitutive model of reinforced concrete[3]

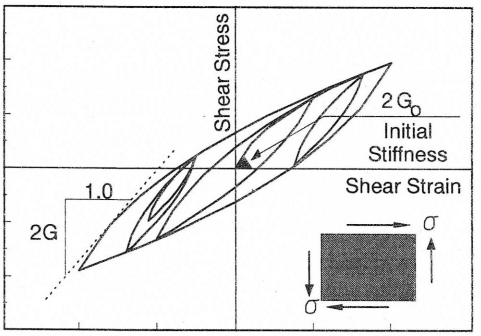

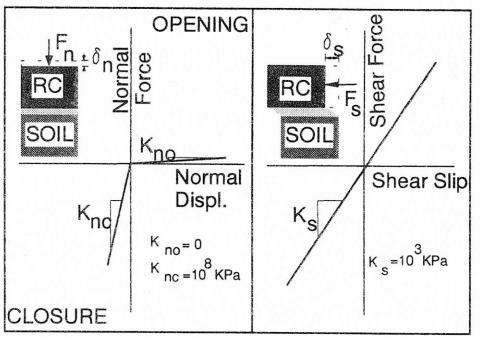

Fig.1b Computed shear stress-strain relation for soil[6]

Fig.1c Normal and shear relations for RC/soil interface model[6]

3. COMPUTATION TARGET

Typical damage experienced in Kobe in 1995 was the failure of middle columns in underground RC box culverts. Of the 264 RC columns along a subway line, 139 were damaged and 118 collapsed completely. In this study, one typical section of a station is chosen as the target for a collapse simulation and for evaluation of seismic resistance performance. The scenario of failure and final collapse of these structures is of great interest to the authors.

3.1 Failure observations

Diagonal shear cracks were clearly observed in the middle columns of the station. Heavy damage was identified in upper deck columns located in the middle of the underground frame spans, and subsidence of the top slab occurred because the columns were unable to carry the dead load after shear failure (**Fig.2a**). Observations indicated that the maximum subsidence reached 5cm. But for the lower deck columns, the damage was not so serious that they reached ultimate failure. Only few diagonal shear cracks in the columns were seen (**Fig. 2b**). Thus the typical failure in this RC structure was the collapse of middle columns accompanying shear crack and damage to the upper-level columns of the double-deck frames.

Fig.2a Collapse of a column at the upper level

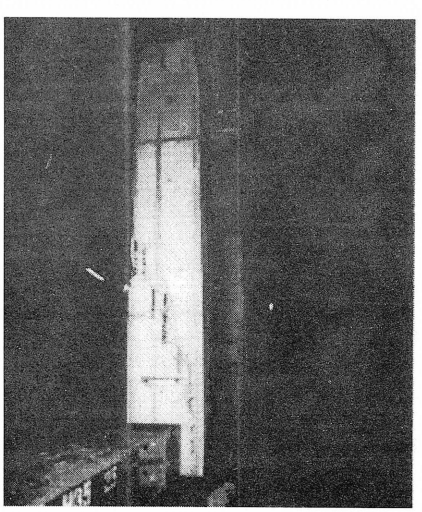

Fig.2b Shear cracks of a column at the lower level

3.2 Layout and structural details

Figure 3a shows the overall shape and dimensions of a section through the station[1,2]. As mentioned, there are two floors to the RC box-type culvert and there is a raw of RC columns on each level. In this section, the spacing of columns is 5m. The outer dimensions of RC underground culvert are 16.68m (width) by 13.25m (height). The wall thickness is 0.8m at the upper floor and 1.0m at the lower floor. The top slab is 1.0m thick and the bottom slab 1.3m thick. The thickness of the middle slab is 0.6m. The middle columns have a cross section of 0.7m x 1.4m at the upper level and 0.6m x 1.5m at the lower level with an average reinforcement ratio of 6.0%. The columns are idealized, being completely fixed to the slabs both in reality and in computation. The station is in soil with an overlay of 5m. The system for dynamic simulation of this underground structure comprises both the 2D RC frame and the surrounding soil.

Figure 3b shows the reinforcement arrangement in the station section under consideration. The middle columns, which suffered serious damage in the earthquake, feature heavy reinforcement in the longitudinal direction with little web reinforcement. The longitudinal reinforcement ratio is 5.1% for the upper columns and 5.7% for the lower columns. The web reinforcement ratio is only 0.075%–0.15%. This not enough to provide substantial shear reinforcement. **Figure 5** and **Table 1** show details of the surrounding soil layers. In computation, the input seismic acceleration was applied at the base of layer 6 since the stiffness of layer 7 is assumed to be large enough for it to be regarded as a rigid engineering boundary for computational purpose.

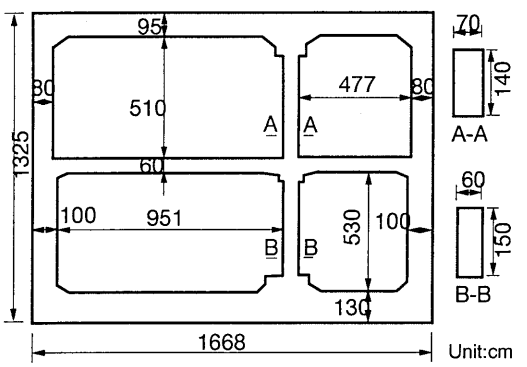

(Column spacing = 5m)

Fig.3a Dimensions of target RC frame

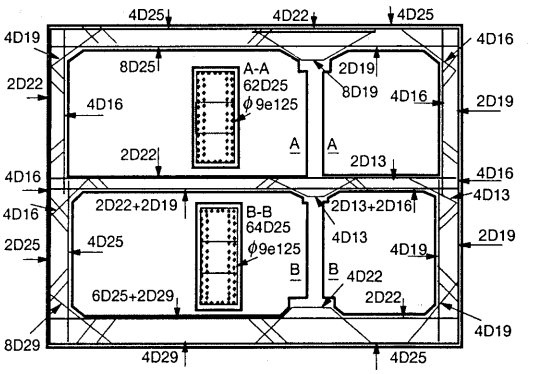

(Steel bars /m)

Fig.3b Reinforcement arrangement of target RC frame

3.3 Input ground acceleration

The earthquake motions used as inputs were recorded at Kobe meteorological observatory and other sites as shown in **Fig.4** and **Fig.29** in a later section. Both horizontal and vertical acceleration records are used to simulate the dynamic response of this soil-RC box system with its longer dimension along the axis of the subway line. It must be noted that these seismic inputs are not the most suitable inputs on the foundation rock but mere records obtained at the ground surface after magnification by propagation through the soil.

Since the authors are unable to produce the highly reliable seismic wave for at the actual site, magnified ground surface waves are used as a substitute for the base rock accelerogram. This makes it difficult to investigate the real cause of the destruction which actually occurred. However, it may be possible to investigate intrinsic structural performance under severe seismic loading and examine the applicability of coupled structural failure analysis and soil foundations. Thus a major aim of this paper is to focus on structural considerations and check computational capabilities. At future stage, joint research with those in the seismic field should follow this structural oriented investigation.

To check seismic performance of existing structures, it is necessary to define the suitable seismic motion and material properties to check since the purpose of verification is the actually attained performance.

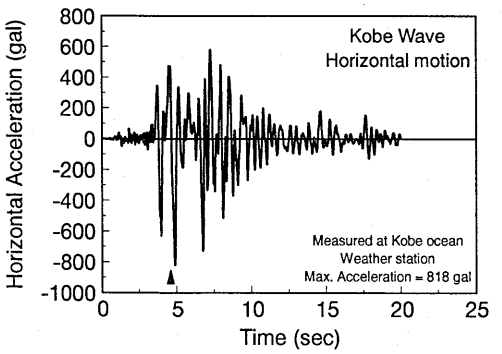

Fig.4a Horizontal acceleration used

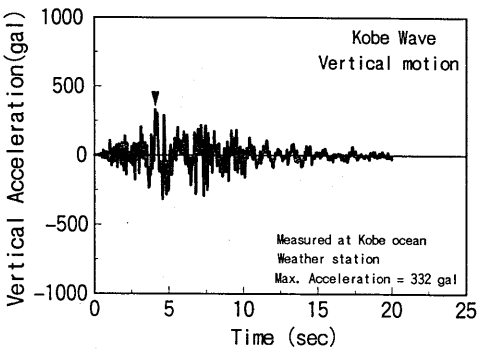

Fig.4b Vertical acceleration used

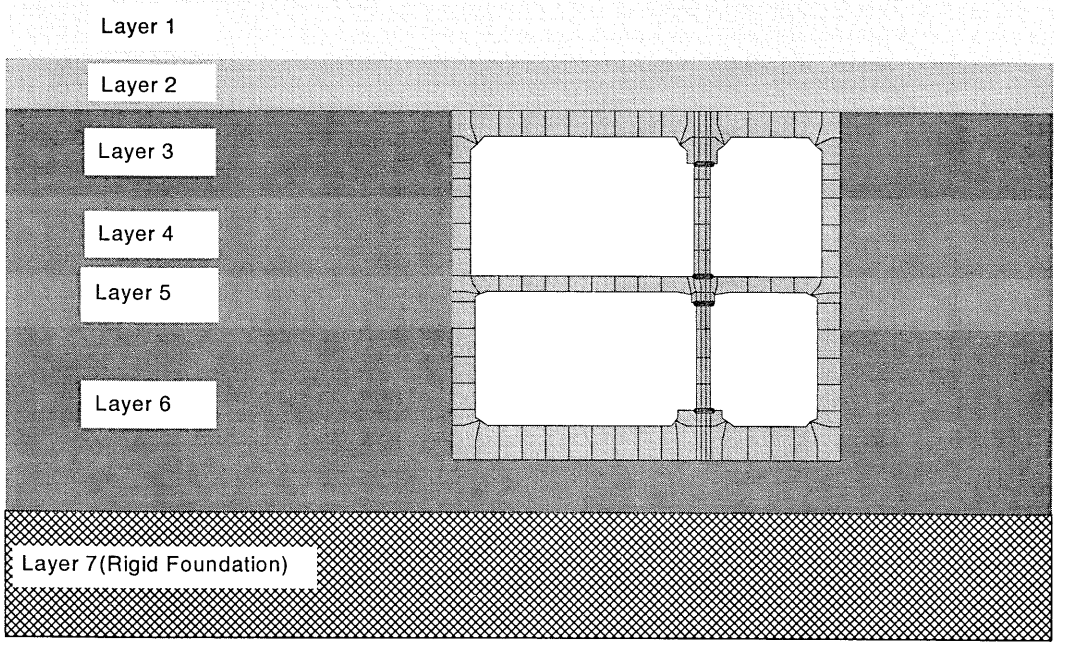

Fig.5 Soil profile around structure

Table 1 Characteristics of surrounding soils

	Layer 1	Layer 2	Layer 3	Layer 4	Layer 5	Layer 6	Layer 7
Layer thickness(m)	3.0	2.0	3.25	3.0	2.0	7.0	>10.0
SPT-N	10	18	20	15	30	42	50
Vs (m/s)	205.0	246.0	256.6	228.7	301	345.3	410.7
Gs (kgf/cm^2)	757.1	1212	1318	1047	1823	2386	2840
Es (kgf/cm^2)	2196	3514	3822	3037	5288	6921	8240
Density (t/m^3)	1.8	2.0	2.0	2.0	2.0	2.0	2.0
Soil Type	clay	sand	clay	sand	clay	clay	clay

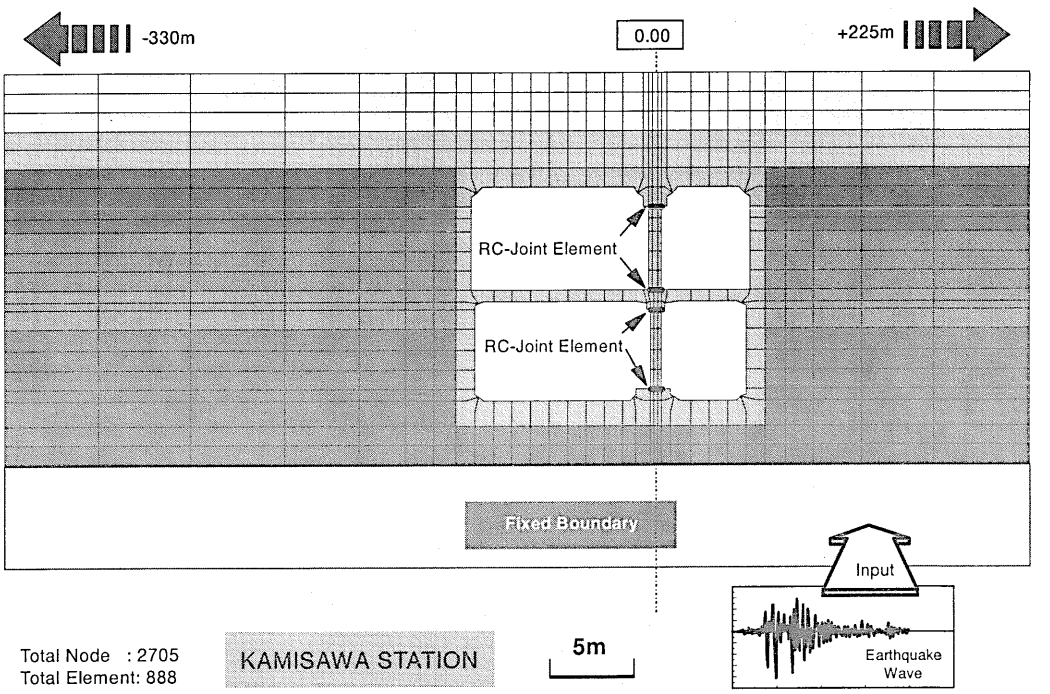

Fig.6 Central part of the finite element mesh of soil-RC system used in FEM analysis

3.4 FEM mesh for RC frame and foundation

The finite element discretization is shown in **Fig. 6**. Higher-order isoparametric elements are used to analyze the target section. In flexure, only one layer of higher-order elements is necessary and sufficient. In shear, however, several layers are required since shear strain develops nonlinearly over the thickness of members, unlike flexural normal strains[8]. Thus, three layers are placed at the middle columns, and mesh sensitivity and convergence were checked in advance. Since the RC outer frame and the columns are of different thickness, the stiffness changes sharply near the joint plane. In order to account for the discontinuous deformation in joint area, RC joint elements are placed between the column and slab. The two extreme sides of the analysis domain are modeled as mixed artificial boundary elements to simulate far-field soil layers[8].

4. COLLAPSE SIMULATION

The coupled behavior of the underground RC structure and the surrounding soil system under the influence of the Kobe earthquake motion was computed using **WCOMD-SJ**[3]. The results as given below show the behavior of the system under seismic loading and the forces induced on the middle columns.

4.1 Inelasticity of the whole RC structure[8]

In order to indicate the level of damage to the entire RC structure in terms of ground water leakage resistance after the earthquake, crack width oriented inelastic output in the time domain is needed. The first strain invariant denoted by (I_1) is closely associated with crack occurrence and the expansion of in-plane elements (volumetric change of the elements)[8]. The mean strain invariant denoted by (I) can be defined as the spatial average value of (I_1) for all RC elements. It is equal to zero in the case of elastic shear behavior, as no volumetric change and no residual deformation exist under pure elastic shear deformation. Hence the mean strain invariant (I), called inelastic strain, can be used to represent the magnitude of damage to the reinforced concrete. The value of (I) can be calculated as follows.

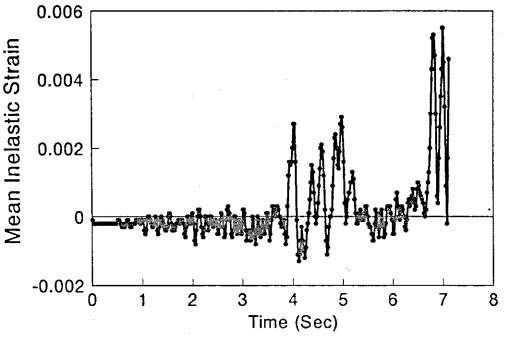

Fig.7 Inelastic strain representing RC damage in the time domain

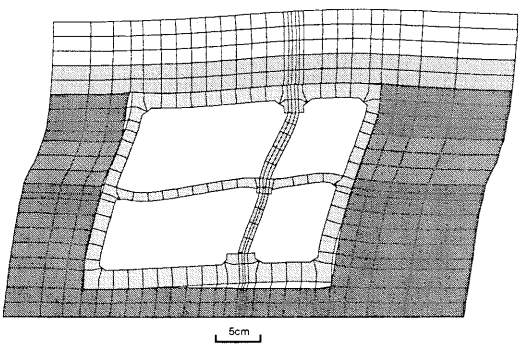

Fig.8a Deformation profile of RC-soil system just before failure

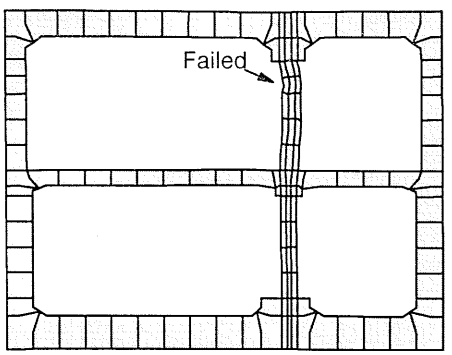

Fig.8b Deformation profile of station at failure

$$I = \sum_{allelements} I_1(x,y)dx \cdot dy / A, \quad I_1 = \frac{\varepsilon_1 + \varepsilon_2}{2} \tag{1}$$

where, ε_1 and ε_2 are the 2-D principal strains at (x,y) and A is the total area of the RC in-plane elements.

Figure7 shows the inelastic strain (I) of the target RC frames in the time domain. This index is used to qualitatively determine how much damage is caused to the RC structure and how much deformation remains after the action. In this figure, we can see an enormous increase in inelastic strain at 7.32 sec, and the structure reached failure at this time.

4.2 Dynamic response of the underground RC

Figure 8a illustrates the deformation profile (magnified) of the RC-soil system at the maximum response just before RC failure in shear. The maximum deformation at the top column is about 0.6% by average shear. Also **Figure 8b** shows the deformation profile of the station at failure. It can be seen that the deformation is concentrated on the upper middle column, which was the actual failure location of the entire RC structural system.

4.3 RC frame crack pattern

In order to confirm the failure location and the failure mode, the crack pattern of the structure just before the failure is shown in **Fig.9a**. **Figure 9b** indicates the cracks in the process of propagating as failure takes place. From **Fig.9a**, it is clear that the large cracks are concentrated in the upper column, whereas, the lower column and other parts of the frame have small cracks only. All cracks shown in **Fig.9b** occur in the last stage of failure. We can see very clearly that large shear cracks developed in the upper column, crossed the section of the column, and ultimately caused the failure. These crack patterns look fairly realistic when compared with the observed cracks shown in **Fig.2.**

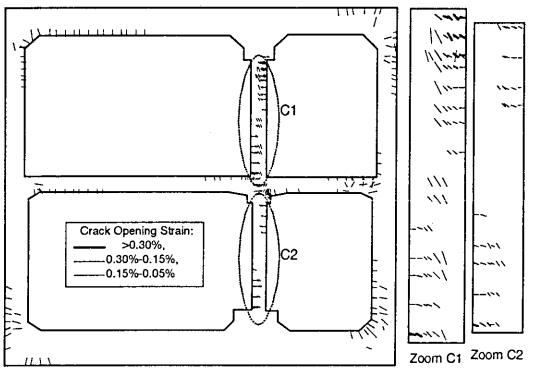

Fig9a Crack pattern of structure just before failure

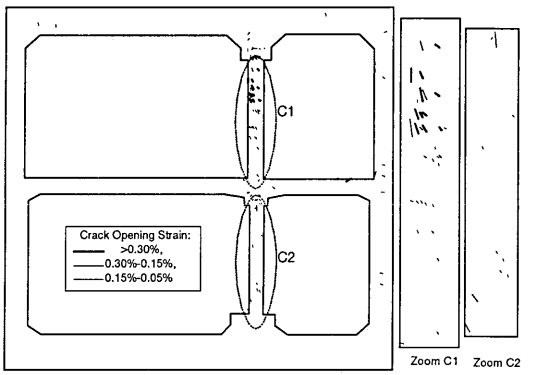

Fig.9b Cracks developed at the failure

4.4 Internal stresses in the middle column

Computational results and observation show that major failures occurred at middle columns. It is important to discuss the forces induced and their ductility in the internal columns. **Figure 10** shows the internal nominal stresses (axial compression and shear divided by the cross-sectional area of members) and the ductility of the column for both upper and lower parts.

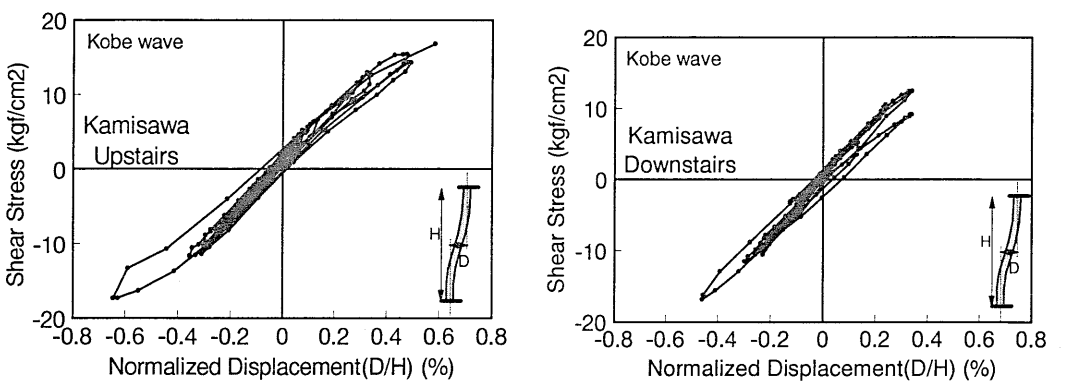

Fig.10a Shear stress-displacement relationship for columns

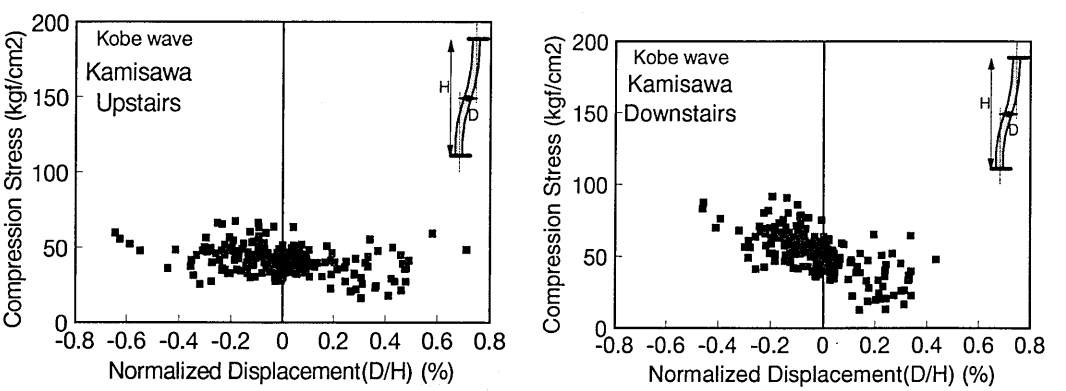

Fig.10b Compression stress variation of the columns

Figure10a shows the relation between the nominal shear stress (shear force normalized by the cross-sectional area of a member) and the relative displacement between top and bottom of the column. The relative displacement is also normalized by the height of the column. The column fails at a maximum normalized displacement of 0.7% and a maximum shear stress of 18kgf/cm^2. The lower column is subjected to similar nominal stress with a slightly smaller shear displacement and no failure takes place.

Figure 10b shows the changes of nominal compressive stress in the columns. It can be seen that the compressive stress varies between 20kgf/cm^2 and 70 kg/cm^2 due to the up-and-down motion of the earthquake. The maximum compressive stress is less than 100kgf/cm^2, and which is well below the compression capacity of the RC columns.

4.5 Collapse mechanism study

According to an FEM simulation of the failure mechanism, the RC columns would lose axial load carrying capacity after the occurrence of the localized diagonal shear cracks occurred, and this would be followed by sudden failure of the outer frame. Some cracks would be introduced in the lower column and the corner of the RC box but the damage level would be lower.

The aim of this dynamic analysis of an RC underground structure is to look into a rational seismic resistant design method based on knowledge of the collapse mechanism. As most of the damage to this underground RC has its roots in the diagonal shear failure of the middle column[9], the shear behavior of the RC columns will be checked against the shear capacity equation in the JSCE code[10] as,

$$V_c = V_{cd} + V_{sd} \tag{2}$$

where, V_c is the shear capacity of the RC member; V_{cd} is the shear force carried by the concrete and longitudinal reinforcement; and V_{sd} is the shear force carried by the web reinforcement. V_{cd} and V_{sd} can be evaluated using the following formulas:

$$V_{cd} \propto (\rho_l)^{\frac{1}{3}} (f_c')^{\frac{1}{3}} (d)^{-\frac{1}{4}} \qquad V_{sd} \propto \rho_w \tag{3}$$

where, ρ_l is the reinforcement ratio of longitudinal bars; ρ_w is the reinforcement ratio of web steel; f_c' is the compressive strength of concrete; and d is the effective depth of the RC member.

From these equations, the shear capacity of the upper column can be calculated. If no axial force is considered, the shear strength of this column is 14.6kgf/cm^2. As the compression force varied from 10kgf/cm^2 to 100kgf/cm^2 in the esponse to the earthquake motion, the shear capacity reaches a maximum of 17.2kg/cm^2 when the axial compression force is taken into account. The FEM computation above indicates that shear stress in the upper column can reach 18kgf/cm^2, a little bit higher than the shear strength.

Another aspect of the seismic resistance capacity of an RC member is its ductility. In order to avoid sudden failure,an RC member should be designed to fail after its of longitudinal reinforcement yields. In the dynamic simulation of the underground RC, it was found that the middle column failed before or just after longitudinal bars yield. This has also been pointed out by 3-D FEM analysis[9]. Thus it is necessary to discuss the ductility of the columns in RC frames. The ductility level of an RC member can be estimated by

$$\frac{V_c}{V_y} \geq N = N_{rq} \tag{4}$$

where N is a factor reflecting the ductility of the RC member. If N is less than unity, the member behaves with a brittle mode of failure. V_y is the shear force corresponding to the bending capacity denoted by M_y (**Fig.11**), and is defined as the yield shear force here. Then, V_y can be calculated as,

$$V_y = \frac{My}{H/2} \propto \rho_l \tag{5}$$

where H is the height of the column.

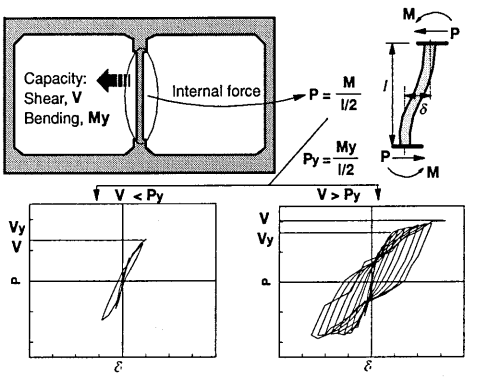

Fig. 11 Relationship between shear capacity and ductility

In the case of the upper columns in the underground RC structure considered here, the bending capacity is more than 410 ton-m when the longitudinal bars yield. The shear force at this time is about 20kgf/cm^2. The ductility factor N is then 0.73, which is much smaller than unity. Certainly, the middle column ductility is less with diagonal shear cracking.

In evaluating seismic resistance, both shear capacity and ductility should be considered. From **Eq.(2)**, it seems that for RC members with ordinary concrete strength, there are two ways to increase the shear capacity; one is to increase the amount of longitudinal reinforcing bars, and the other is to enhance the web reinforcement (See **Fig.11**).

In the first case, the bending capacity, defined as M_y will be simultaneously increased. As the bending capacity corresponds to the yield point of the main reinforcing bars, the shear force V_y at the moment of yield becomes very large, as calculated by **Eq.(5)**. The shear capacity will also increase according to the JSCE code as,

$$V_c \propto (\rho_l)^{\frac{1}{3}} \tag{6}$$

According to **Eq.(5)** and **Eq.(6)**, the yield shear force generally increases more than the shear capacity as the amount of main reinforcement rises. RC members with this kind of reinforcement arrangement are very brittle, and fail suddenly without much ductility. The failure of the middle columns in this subway stations falls into this category.

On the other hand, if the shear capacity is increased by enhancing the web reinforcement, the shear capacity V will be greater than the yield shear force V_y. The ductility of the RC member will thus be higher. RC members with higher shear capacity generally exhibit better seismic resistant performance.

5. ENHANCEMENT OF RC SEISMIC PERFORMANCE

As discussed above, the shear capacity of the columns in the underground RC is found to be lower so they had low ductility. In order to enhance the seismic resistance of RC structures in general, improvements to both shear capacity and ductility are effective.

However, the capacity of middle columns of underground box sections has hardly any influence on the overall shear deformation of the RC structure and the induced sectional forces, because structural deformation is closely associated with interactions with the soil foundation. Since the main performance requirement of the columns is to sustain vertical forces no matter how large the shear deformation occurs in the box section. For underground RC structures, member ductility is a primary focus in the design of new structures and the retrofitting of existing RC structures. Thus, the ratio of shear capacity to flexure will be of great interest to us.

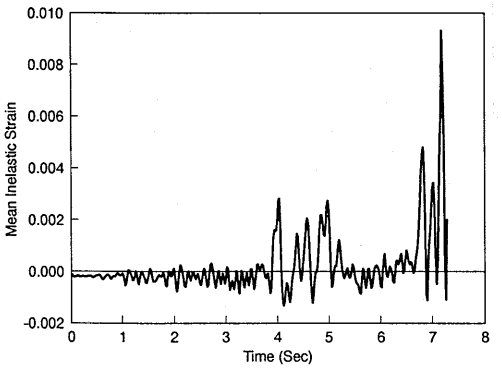

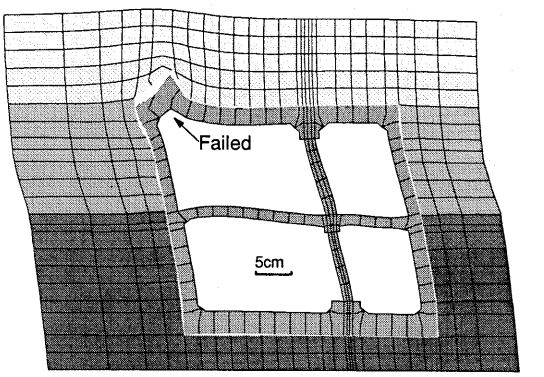

Fig.12 Inelastic strain representing damage in time domain **Fig.13** Deformation profile of RC-soil system at failure

5.1 Increase in web reinforcement ratio in middle columns

Computations are based on the same RC frame as used in the previous section. The amount of web reinforcemnt in the column is increased to 0.76% (D16 with spacing of 7.5cm; volumetric ratio is 1.66%) , and the shear capacity reachs 33.3kgf/cm^2 according to the shear equation of JSCE code (with no consideration of axial compressive force). As no change is made in longitudinal reinforcement arrangement, the yielding shear force V_y is still 20kgf/cm^2. The shear capacity to flexure capacity ratio N is 1.67. In this case, the columns are expected to have sufficient shear resistance against seismic action.

a) Inelasticity of the whole RC structure

Figure 12 shows the inelastic strain *(I)* in this enhanced shear case in the time domain. In this figure, we can see that the structure fails at 7.32 seconds.

b) Dynamic response of the RC frame

Figure 13 shows the deformational profile of the station at failure. It can be seen that deformation is concentrated at the corner of the RC outer frame, and that failure took place at the upper slab. Since there is just one finite element layer, the possibility of failure will be again checked in terms of shear forces developed. There is no localization of deformation in the columns, since the middle column is strongly reinforced in shear.

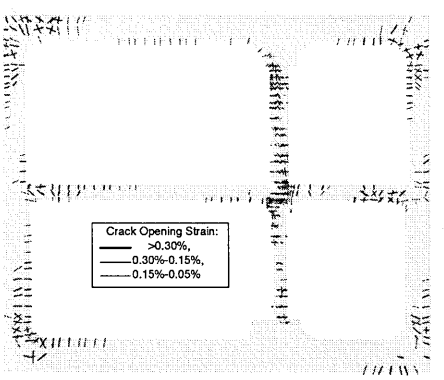

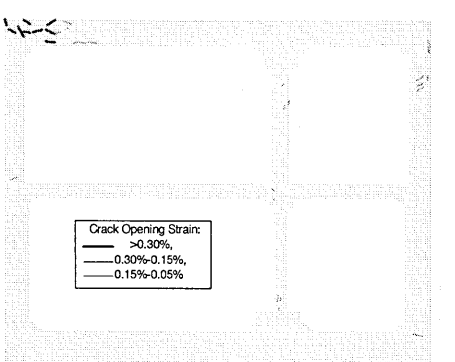

Fig.14a Crack pattern of structure just before failure **Fig.14b** Cracks developed at failure

c) Crack pattern of the RC frame

To identify the failure location and failure mode in this case of a column greatly reinforced against shear, **Figure 14a** shows the crack pattern of the structure just before failure. Large cracks are seen in several places, such as in the upper column, in the lower column, in the middle slab-column joint and at the corners of the frame. **Figure 14b** shows the cracks which developed at failure. All racks shown in **Fig.14b** are introduced in the last computational step. Only distinct shear cracks within the upper slab, near the left corner, can be seen crossing the section of this column. Thus the shear is brought to a focus at the upper slab near the corner.

d) Internal stresses in middle columns

The computational results for the enhanced shear reinforcement case indicate that collapse takes place not at the middle column but in the left corner of the upper slab. Discussion of the forces induced in the internal column may be advisable to further clarify the failure section in the slab.

Figure 15 shows the relation between nominal shear stress and relative shear displacement of the upper and lower columns. The relative displacement is normalized by the height of the column. For the upper column, when the failure occurs, the shear stress in the column is small. The maximum normalized displacement is 0.5% and the maximum shear stress is 18kgf/cm^2.

On the other hand, the lower column experiences shear stress of 12kgf/cm^2 and no failure takes place. There is not much difference between **Fig.10a** and **Fig.15**, but a large difference in failure mode. The shear capacity is greatly increased in this case, but the ductility response remains unchanged as the main reinforcement remains constant and has a large absolute value.

e) Internal stresses in the slab corner

Figure 16 shows the changes in shear stress in a section at the corner. It can be seen that the shear stress reaches 18kgf/cm^2 just before failure. The estimated shear capacity of this slab as given by the of JSCE code[10] is 15.2kgf/cm^2. Thus, the slab is supposed to fail in shear.

f) Collapse mechanism of subway station

In the shear enhanced case, the FEM simulation indicates that the middle RC columns are strong enough to resist shear and will not fail under the earthquake motion. However, the overall structural performance improves little as the main reinforcement ratio remains unchanged. Thus, this partial strengthening merely results in a shift of the weakest point.

5.2 Reduction of main reinforcement for improving ductility

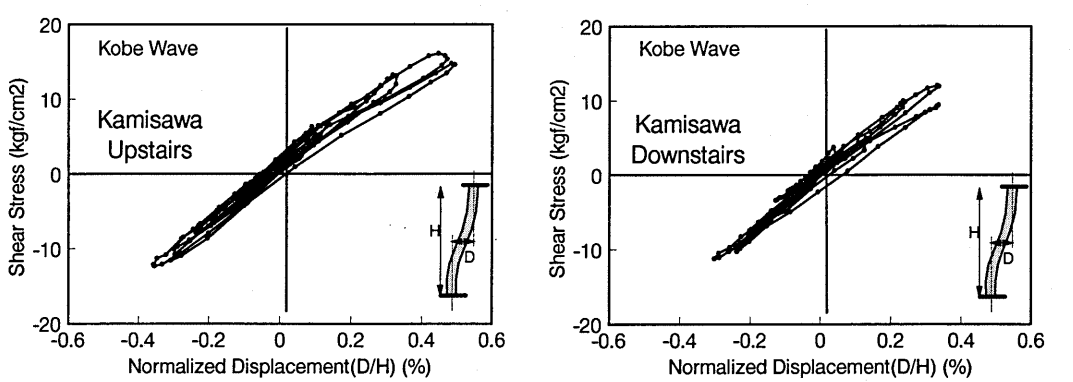

Fig.15 Shear stress-displacement relationship for columns

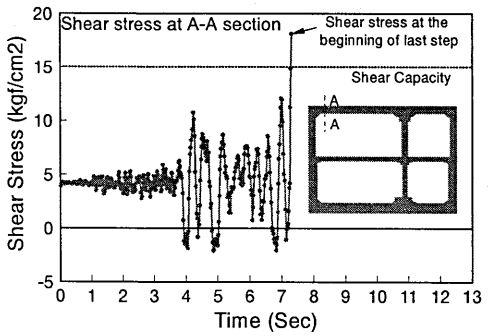

Fig.16 Shear stress variation at the failure section

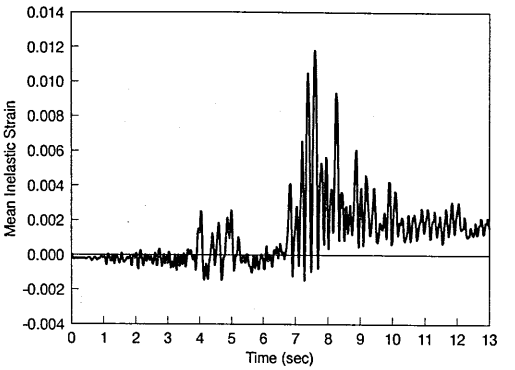

Fig.17 Inelastic strain representing damage in time domain

A computation was carried out on the same RC frame in which the web reinforcement ratio of the column was increased to 0.76%. In this case, though, the longitudinal reinforcement ratio is made 3.67%, in an attempt to enhance the ductility of the columns. The shear capacity then increases to 32.1kgf/cm^2 according to the JSCE code. The main reinforcement ratio is also reduced so as to obtain yield shear stress of 14.4kgf/cm^2, equivalent to yielding of the main steel. The shear/flexure capacity ratio N reaches 2.23 in this case. Thus, considerable ductility is achieved along with sufficient shear capacity.

a) Inelasticity of the whole RC structure

Figure17 shows the inelastic strain (I) in the enhanced shear and reduced flexure case in the time domain. This demonstrates that the structure does not fail at any stage during the seismic motion.

b) Internal stresses in the middle column

Figure 18 shows the relation between nominal shear stress and relative displacement. The relative displacement is normalized by the height of the column. For the upper column, the maximum normalized displacement reaches 1.2% and the maximum shear stress 18kgf/cm^2. On the other hand, the lower column is subjected to a shear stress of 12kgf/cm^2. By the comparing this figure with **Fig.11a** and **Fig.15**, the improved ductility accompanying the flexural nonlinearity can be clearly identified.

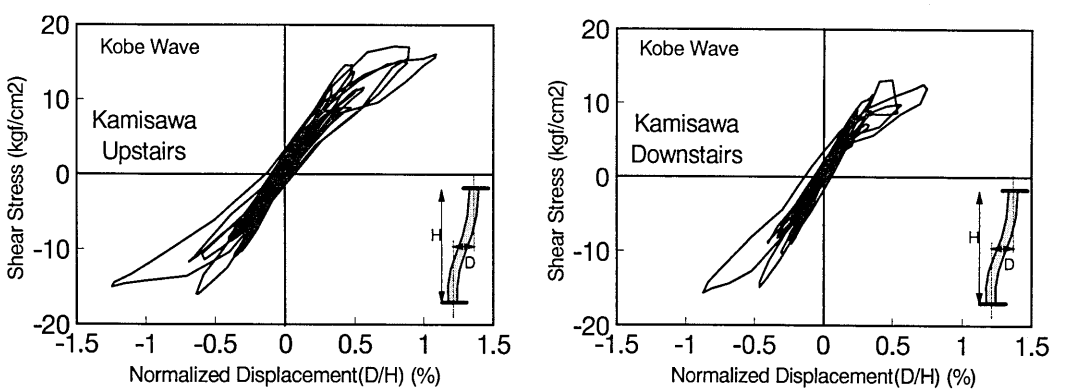

Fig.18 Shear stress-displacement relationship for columns

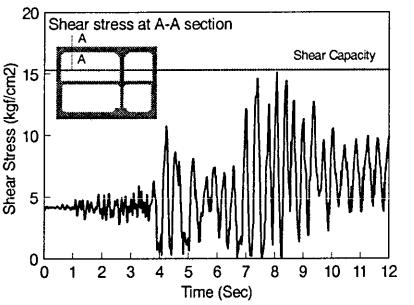

Fig.19 Shear stress variation at the corner section

c) Internal stresses in slab corner

In order to compare this high ductility case with the previous one, the changes in shear stress in a section at the corner, where the failure took place in the enhanced web reinforcement case, is shown in **Fig.19**. The maximum shear stress is reduced to 15kgf/cm^2 by reducing the flexural capacity but elevating the ductility of the structure.

5.3 Summary of the parametric computation

The three parametric computation cases are summarized in **Table 2**. These trial computations show that both shear capacity and ductility are important factors in seismic resistant performance. An RC member with low shear strength will fail in shear mode under seismic loading, while an RC structure with a higher shear strength and ductility can survive an earthquake. This computational experience teaches us that a ductile structure possesses higher seismic resistance.

Table 2 Parametric study on member ductility

Case	Original	Enhanced web	Enhanced web +reduced flexural
Main reinforcement ratio	5.1%	5.1%	3.67%
Web reinforcement ratio	0.15%	0.76%	0.76%
V (kgf/cm^2)	14.6	33.3	32.1
V_c (kgf/cm^2)	10.0	10.0	8.8
V_s (kgf/cm^2)	4.6	23.3	23.3
V_y (kgf/cm^2)	20	20	14.4
N	0.73	1.67	2.23
Failure location	upper column	upper slab	no failure

6. SOIL STRUCTURE AND SEISMIC MOTION

The dynamic system discussed above includes the underground RC structure and the soil foundation. A change in the reinforcement ratio of the RC frame proved to be a very effective means of damage control. In this section, aspects of the interaction with the soil foundation and wave characteristics will be studied for an enhanced understanding of the behavior of the whole dynamic system.

6.1 Soil profile

In the original case of Kamisawa station, soil properties vary in the vertical direction. The shear modulus of the soil is specified as larger as depth increases. **Figure 20** shows the original soil profile. The soil around the

upper deck is softer than that around the lower deck. Since the softer soil may allow greater induced shear deformation of the RC culvert, greater shear deformation can be expected in the upper columns under the earthquake loading. This may be the reason why columns failed on the upper floor while those on the lower floor had just a few shear cracks.

The effects of the soil profile can be checked by changing the soil profile used in the computation. If the failure mode and position are found to be affected by a change in soil profile, then soil structure would be shown to have a considerable influence on failure mechanism. Thus a computation is performed with a different soil profile from the original case, that is, the foundations around the RC frame are taken as a single material with a shear modulus of 1318 kgf/cm^2, which is similar to that of layer 3 in the original case. Other factors are as in the original computation. The computational results for this modified soil profile are shown in **Fig.21** to **Fig.24**. The inelastic strain of the RC box in the time domain is shown in **Fig.21**. By comparing **Fig.21** with the original case (**Fig.7**), much difference of the response is identified. The structure failed at 5.2 sec with an abrupt increase in the structural damage. As the mean shear modulus of the original case was 1603 kgf/cm^2, premature failure would be associated with soft foundations.

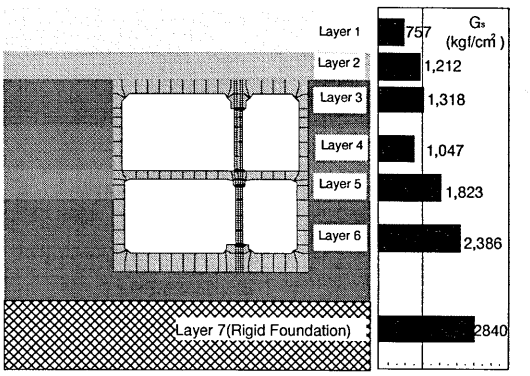

Fig.20 Assumed shear modulus profile for soil foundation

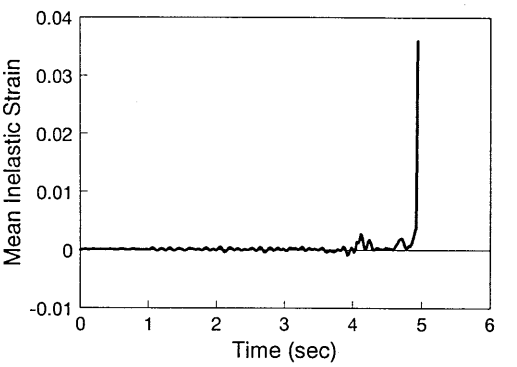

Fig.21 Inelastic strain representing damage in time domain

The next point of interest is the location of failure. **Figure 22** shows the deformation profile of the RC frame under the excitation. In **Fig.22a**, which shows the deformation profile just before failure, greater deformation of the lower column is seen than in the original case (**Fig.8a**). In order to focus on the failure position more clearly, the deformation profile of the station at failure is shown in **Fig.22b**. Deformation is concentrated in the lower column. Thus the failure position has changed from the upper to lower level when the soil profile is made uniform.

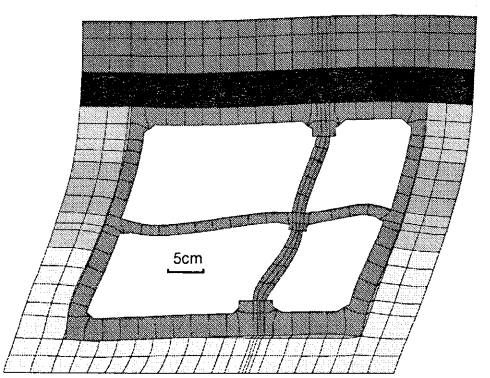

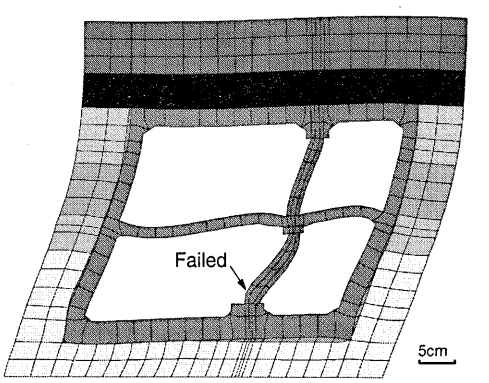

Fig.22a Deformation profile of RC-soil system just before failure

Fig.22b Deformation profile of station at failure

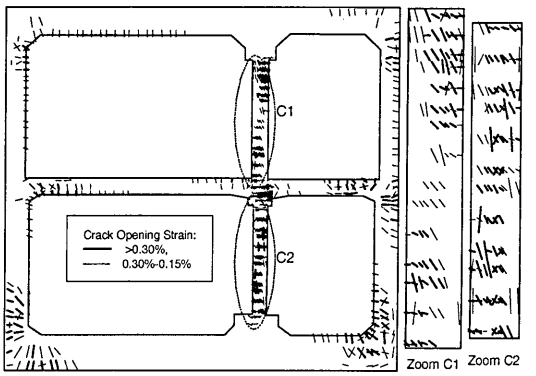

Fig.23a Crack pattern of RC frame just before failure

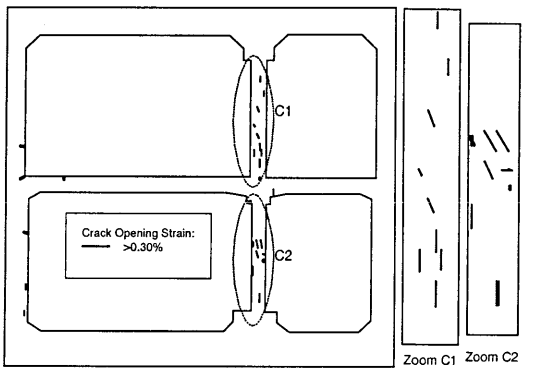

Fig.23b Cracks produced at failure

The crack pattern shown in **Fig.23a** supports this discussion of the failure location. There are many cracks in the two columns, in contrast with **Fig.9**. The damage is much heavier than in the original case (**Fig.9a**). **Figure 23b** shows the cracks that develop in the last step. Diagonal shear failure and cracking are clearly detected.

Figure 24 shows the internal shear stresses and shear deformation of the columns in both upper and lower parts of the frame. Considerable shear deformation takes place in the lower column, which ultimately failed. The shear stress is also higher in the lower column than in the upper one.

All these computational results clearly demonstrate that the soil profile will affects the damage occurring to the RC underground structure. It also shows that the soft foundation soil around the upper deck of the frame contributed to the observed damage to the upper columns. The magnitude of shear deformation in soil-RC coupled systems is shown to be determined by a combination of wave characteristics, structural stiffness and soil stiffness. As this demonstrates very well, the entire system has to be modeled in the seismic design of underground structures.

6.2 Effect of vertical seismic motion

One of the characteristics of the input seismic motion used in the above discussion is that the vertical component is rather high. In fact, the maximum vertical acceleration reached about 40% of the maximum horizontal accelercation. In general, the vertical component of seismicity is ignored owing to its small contribution to structural safety issues and dynamic response of the structure. However, influenced structural behavior was reported[11] even when the vertical ground motion is cut off in the dynamic computation. So it is meaningful to discuss the influence of the vertical ground motion, especially in the cases where failure of the column does not occur.

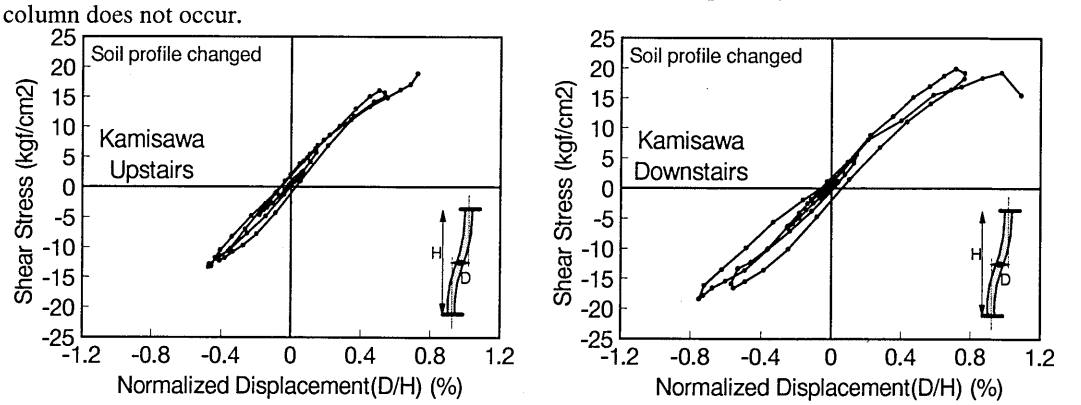

Fig.24 Shear stress-displacement relationship for columns

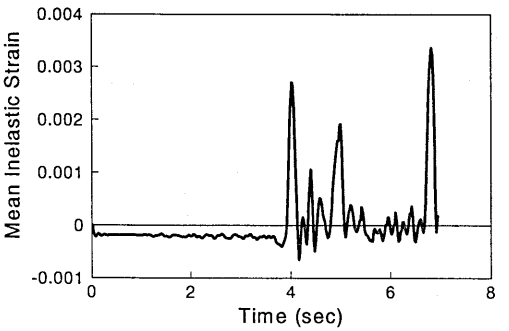

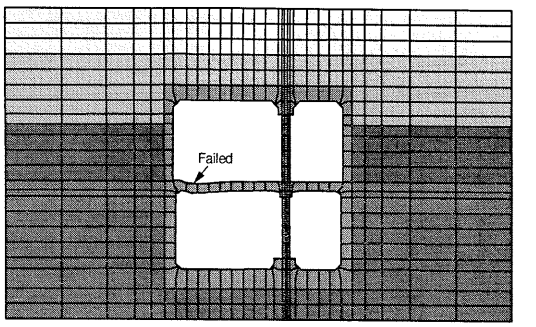

Fig.25 Inelastic strain representing damage in time domain

Fig.26 Deformation profile of station at failure

In section 5.1 the case of a heavily shear reinforced column was discussed. and failure was found to take place in the upper slab. Here, the computation will be repeated for this case but with the vertical component of ground motion completely cut off.

The computed results under no vertical motion are summarized in **Fig.25** to **Fig.28. Figure 25** shows the inelastic strain in time. The structure failed at 6.96 seconds.

In order to identify the failure position more clearly, the deformation profile at failure is shown in **Fig.26.** It can be seen that the deformation is localized in the left side of the middle slab.This means that the point of failure shifts from the upper slab to the middle slab if the vertical component of ground motion is ignored.

It is necessary to check the internal stress conditions carefully to confirm the mode of failure. **Figure 27** shows the internal shear stresses and the shear deformation of the column. It can be seen through a comparison with **Fig.15** that the shear strength of the column is barely affected, and only the induced axial compression is influenced.

The shear stress changes at sections A-A and B-B in the upper and middle slabs are shown in **Fig.28.** Section A-A is the point where the slab failed in shear mode in the case of enhanced shear reinforcement only(**Fg.16**). Provided that the vertical motion is removed from the computation, the shear stress in section A-A does not reach failure level (over 15 kgf/cm^2), but the shear stress in section B-B of the middle slab reaches shear capacity (over 9kgf/cm^2). Thus, the structure fails in the middle slab when the vertical ground motion is ignored in the computation.

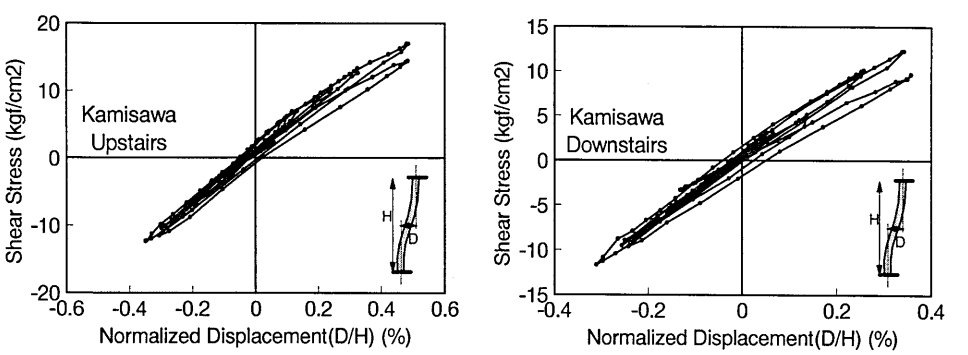

Fig.27 Shear stress-displacement relationship for columns

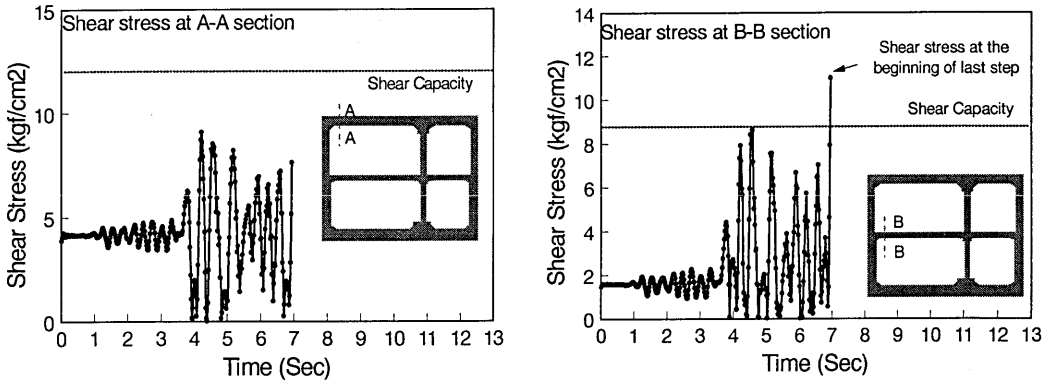

Fig. 28 Shear stress variation in time domain

Even though the vertical ground motion is not a primary cause of failure, the combination of horizontal and vertical motion may affect the dynamic response of the structure as well as the point of failure. The effect of combined vertical and horizontal motion is very complex and needs to be further studied to understand the basis of mechanism.

6.3 Seismic motion characteristics

As stated above, the motion recorded at the Kobe meteorological observatory includes very high horizontal acceleration with a short period. In order to study the effect of the seismic wave form characteristics on the underground structure, two waves forms are used in a dynamic computation (**Fig.29**).

The first is an artificial wave form produced for the Koutouen area, which is based on the earthquake record on solid engineering foundation[12]. The period of this wave is close to that of the Kobe motion used by the authors, while the maximum horizontal acceleration is a little smaller (**Fig.29a**). The second is the seismic motion recorded at Amagasaki city. It combines moderate acceleration level with long-period of motion (**Fig.29b**). The maximum acceleration in both horizontal and vertical directions is similar. **Figure 30** shows the inelastic strain representing the damage level in dynamic response. It can be seen that the target underground structure failed under the artificial Koutouenn wave form but no failure was caused by the Amakasaki motion.

The deformation profile of the RC-soil system when failure occurs is shown in **Fig.31.** This deformation profile is very close to that obtained for the seismic load imposed by the Kobe motion (**Fig.8**). The deformation is also concentrated in the upper columns, where failure actually took place .

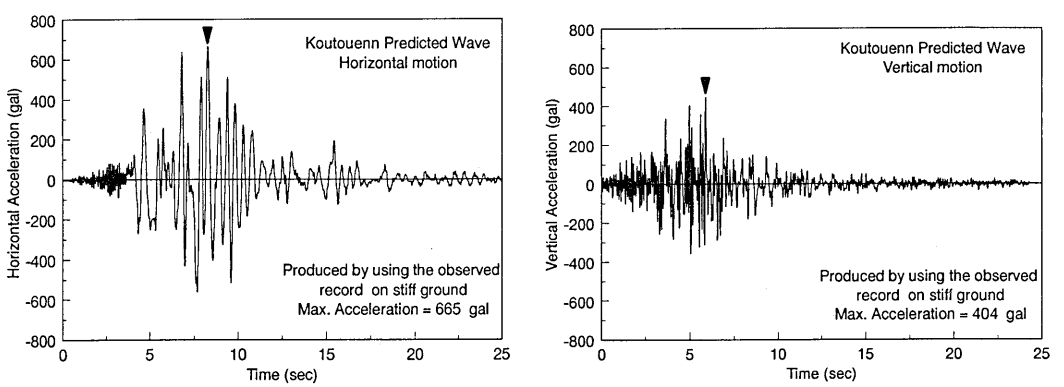

Fig.29a Artificial acceleration profile for Koutouenn area[12]

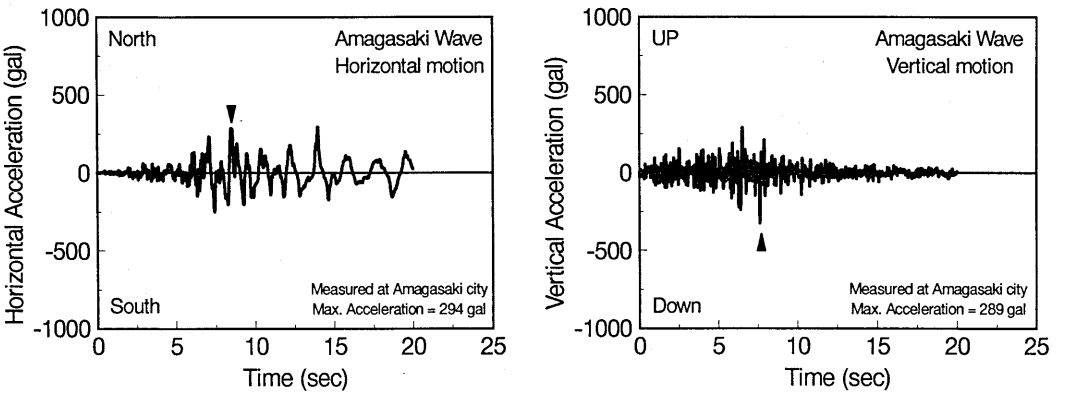

Fig.29b Acceleration records at Amagasaki city

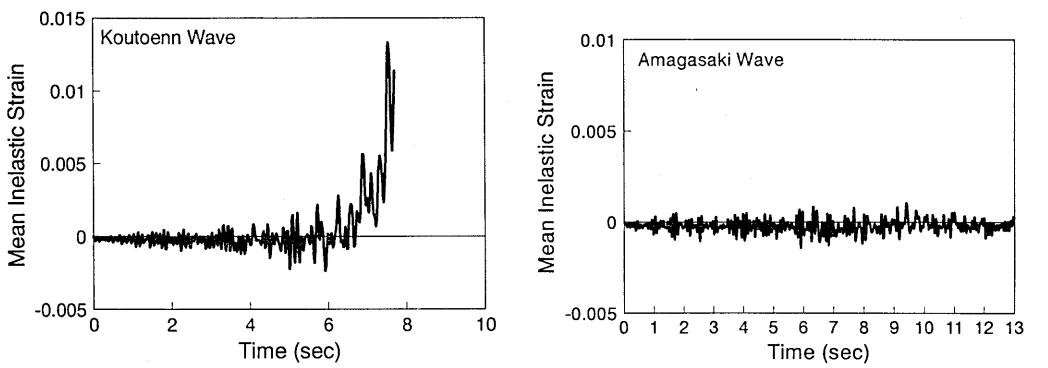

Fig.30 Inelastic strain representing damage in the time domain

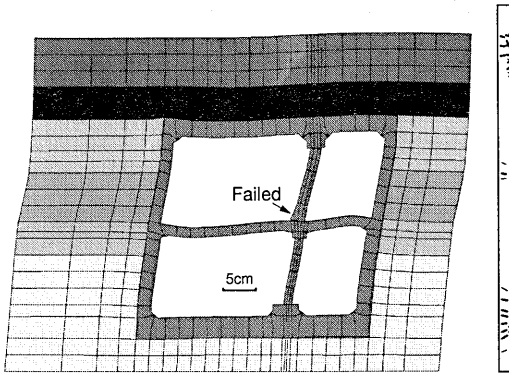

Fig.31 Deformation profile at failure under Koutouen motion

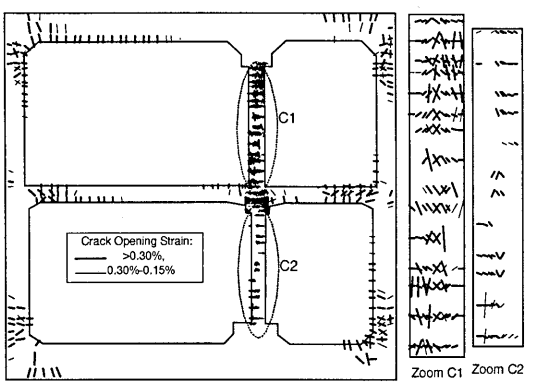

Fig.32 Crack pattern at the failure under Koutouenn motion

The crack pattern at failure is shown in **Fig.32.** The enlargement of the upper column shows many diagonal shear cracks occurring at this time, while only few cracks are introduced in other parts of the RC frame. This situation is also similar to the original case with the Kobe wave form.

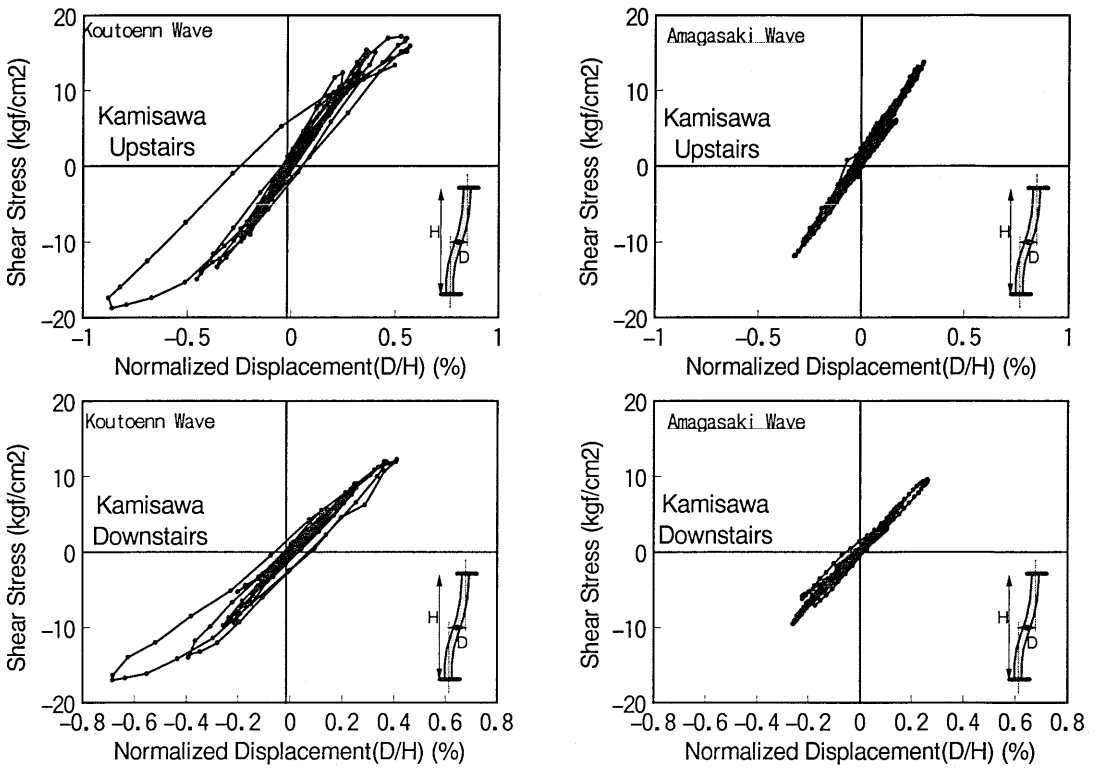

Fig.33 Shear stress-displacement relationship for columns

The internal shear stresses in the middle columns are shown in **Fig.33** for these two cases. Under the seismic load of the Koutouen motion, the shear stress in the upper column rises to nearly 20 kgf/cm^2, and failure occurs. This is similar to the original case with the Kobe wave form(**Fig.10a**). In the case of the Amagasaki motion, the shear stress was less than 15 kgf/cm^2, and no failure occurs in either columns.

Within the limited numbers of input motion stested, a higher acceleration appears to cause the collapse of the middle columns. However, this is not a general conclusion because both wave form characteristics and the mechanical properties of both the RC structure and the foundation soil have an influence on safety. It can be simply concluded that the overall seismic performance of underground RC structures must be estimated in consideration of soil and RC nonlinearities under dynamic motion in both time and space.

6. CONCLUSION

In this study, seven cases of dynamic analysis on an underground reinforced concrete box-section damaged in the Great Hanshin Earthquake were conducted. Group I (**Table 2**), consisting of three cases, was performed to study the collapse.

In group II, the soil profile and the characteristics of the seismic motion were altered and some trial computations carried out, in order to better understand the effect of soil-structure interactions on the dynamic system of an underground RC structures

According to the this analysis, we reach the following conclusions:

(1) Nonlinear models of reinforced concrete coupled with soil nonlinearity can be used as a tool for simulating the collapse of underground structures under seismic loading and evaluating their performances.

(2) The collapse of the subway station studied here is attributable to the low shear capacity and ductility of the middle columns.

(3) The well known and accepted strategy of increasing the shear capacity to enhances ductility and seismic resistance is shown to be effective in the design of underground RC.

(4) The soil profile affects the damage level and failure location. A softer foundation soil may cause greater shear damage.

(5) The combination of horizontal and vertical seismic motions is one factor which affecting the point of failure in existing underground RC structures.

(6) Seismic waves from different sources but with similar period and maximum acceleration give a similar dynamic response. Further discussion is needed on the characteristics of earthquake motion.

ACKNOWLEDGMENT

The authors appreciate the technical advice provided by Dr. A. Shawky of Cairo University, and the kind offer of the seismic acceleration diagram by Dr. Hajime Ouchi of Ohbayashi Corporation.

REFERENCES

1) Samata, S., and Nagamitsu N., Yamamoto, K., and Mori, S. : A study on a failure mechanism of subway station analyzed by a non-linear seismic deformation method, *Proceedings of Technical Conference on the Great Hanshin-Awaji Earthquake, JSCE*, Tokyo, pp.231-238, 1996

2) Tajiri, M., Samata, S., Siba, Y., Sakashita, K., and Watanabe, K. : An analytical study on failure mechanism of a subway station damaged by the 1995 Hyogoken-Nanbu earthquake, *Proceedings of Technical Conference on the Great Hanshin- Awaji Earthquake*, JSCE, Tokyo, pp.239-246, 1996

3) Okamura, H. and Maekawa, K.: *Nonlinear Analysis and Constitutive Models of Reinforced Concrete*, Gihodo, Tokyo, 1991

4) Okamura, H. and Maekawa, K. : Reinforced concrete design and size effect in structural nonlinearity, invited, *Proceeding of JCI International Workshop: Size Effect in Concrete Structures*, Sendai, Japan, pp.1-20, 1993

5) Collins, M.P. and Mitchell, D. *: Prestressed Concrete Structures*, PRENTICE HALL, Englewood Cliffs, New Jersey 07632, pp.345, 1991

6) Shawky, A. and Maekawa, K. : Nonlinear dynamic analysis for underground reinforced concrete structures, *East Asian-Pacific Conference on Structural Engineering and Construction,* EASEC-5, Australia, July 1995

7) Ohsaki, Y. : Some notes on Masing's law and nonlinear response of soil deposits, *Journal of the Faculty of Eng. (B), The University of Tokyo*, Vol. XXXV, No. 4, 1980

8) Shawky, A. and Maekawa, K. : Computational approach to path-dependent nonlinear RC/soil interactions, *J. Material, Concrete. Struct., Pavements,* JSCE, No.532/V-30, pp.197-207, Feb. 1996

9) Tajiri, M., Samata, S., Matsuda, T., and Ouchi, H. : A study on the damage of underground railway structure during the Great Hanshin Earthquake, *Proceedings of Technical Conference on the Great Hanshin- Awaji Earthquake*, JSCE, Tokyo, pp.255-262, 1996

10) JSCE, *Standard specification for design and construction of concrete structure*, pert I(Design), 1st ed, Tokyo, 1986

11) Shawky, A. and Maekawa, K. : Collapse mechanism of underground RC structures during Hanshin Great Earthquake, *Cairo First International Conference on Concrete Structures*, 1996

12) Ouchi, H., Ejiri, J., Matsumoto, N. and Matsuoka, Y. : A study on the Shinkansen viaduct damage during the Great Hanshin Earthquake and seismic performance of retrofitted structure, *Proceedings of Technical Conference on the Great Hanshin-Awaji Earthquake*, JSCE, Tokyo, pp.305-312, 1996